HHS Public Access

Author manuscript

Mol Cell. Author manuscript; available in PMC 2016 February 19.

Published in final edited form as:

Mol Cell. 2015 February 19; 57(4): 721–734. doi:10.1016/j.molcel.2015.01.004.

Stress Induces p38 MAPK-mediated Phosphorylation and Inhibition of Drosha-dependent Cell Survival

Qian Yang[1,2,*], **Wenming Li**[2], **Hua She**[2], **Juan Dou**[2], **Duc M Duong**[3], **Yuhong Du**[2], **Shao-Hua Yang**[4], **Nicholas T. Seyfried**[5], **Haian Fu**[2], **Guodong Gao**[1], and **Zixu Mao**[2,3,*]

[1]Department of Neurosurgery, Tangdu Hospital, the Fourth Military Medical University, Xi'an, Shanxi 710038 China

[2]Department of Pharmacology, Emory University School of Medicine, Atlanta, GA 30322 USA

[3]Department of Neurology, Emory University School of Medicine, Atlanta, GA 30322 USA

[4]Department of Pharmacology and Neuroscience, University of North Texas Health Science Center, Fort Worth, TX 76107 USA

[5]Departments of Biochemistry, Emory University School of Medicine, Atlanta, GA 30322 USA

SUMMARY

MicroRNAs (miRNAs) regulate the translational potential of their mRNA targets and control many cellular processes. The key step in canonical miRNA biogenesis is the cleavage of the primary transcripts by the nuclear RNase III enzyme Drosha. Emerging evidence suggests that the miRNA biogenic cascade is tightly controlled. However, little is known whether Drosha is regulated. Here we show that Drosha is targeted by stress. Under stress, p38 MAPK directly phosphorylates Drosha at its N-terminus. This reduces its interaction with DiGeorge syndrome critical region 8, and promotes its nuclear export and degradation by calpain. This regulatory mechanism mediates stress-induced inhibition of Drosha function. Reduction of Drosha sensitizes cells to stress and increases death. In contrast, increase in Drosha attenuates stress-induced death. These findings reveal a critical regulatory mechanism by which stress engages p38 MAPK pathway to destabilize Drosha and inhibit Drosha-mediated cellular survival.

INTRODUCTION

miRNAs, as a class of powerful modulator of gene expression, play a key role in diverse physiological and pathological processes (Afanasyeva et al., 2011; Lee et al., 1993). The biogenesis of miRNAs consists of several tightly coupled steps. Majority of miRNAs are

*Correspondence: zmao@pharm.emory.edu or qianyang@fmmu.edu.cn.

AUTHOR CONTRIBUTIONS Q.Y., W.L., H.S., J.D., D.M.D, and Y.D. performed the experiments. Q.Y., S.Y., N.T.S., H.F., G.G., and Z.M. designed and analyzed the experiments. Q.Y., W.L., and Z.M. wrote the paper.

SUPPLEMENTAL INFORMATION

Supplemental information includes Six Figures and Experimental Procedures.

initially transcribed by RNA polymerase II as the long primary miRNAs (pri-miRNAs). Nuclear RNase III enzyme Drosha with co-factor DGCR8 (Di George Syndrome critical region gene 8) in the microprocessor complex processes pri-miRNAs into a ~65-80 nucleotide hairpin structure named the precursor miRNAs (pre-miRNAs) (Lee et al., 2003). Following transportation into the cytoplasm by an exportin-5 dependent mechanism, pri-miRNAs are further processed by the second RNase III enzyme Dicer to generate the ~22 nucleotide mature miRNAs. Therefore, Drosha controls the initial step of this evolutionarily conserved process in the nucleus. Recently, Drosha has been shown to function in the cytoplasm to process virus-derived cytoplasmic pri-miRNAs (Shapiro et al., 2012). Although there is considerable understanding of how Drosha recognizes and cleavages pri-miRNAs, little is known how Drosha is regulated.

Emerging evidence indicates that the process of miRNA biogenesis is subjected to complex regulation. Several protein factors involved in miRNA biogenesis are regulated at posttranslational level (Paroo et al., 2009). There are also examples of protein factors influencing miRNA processing under various conditions (Michlewski and Caceres, 2010; Wu et al., 2010). For example, MAPK-activated protein kinase 2 (MK2), acting downstream of p38 MAPK, has been reported phosphorylate Argonaute 2 to facilitate its localization to processing bodies (Zeng et al., 2008) or p68, a co-factor of Drosha complex, to regulate the processing of a subset of pri-miRNAs (Hong et al., 2013). Phosphorylation of DGCR8 by ERK increases its stability and has been associated with a progrowth miRNA expression profile (Herbert et al., 2013). Methyl-CpG binding protein 2 (MeCP2) has recently been shown to bind to DGCR8 and interfere its assembly with Drosha (Cheng et al., 2014). A growing body of evidence suggests that stress conditions and miRNAs are highly intertwined. Stress modulates the expression of mRNA targets and the activities of miRNA-protein complexes, and importantly, causes cells appear to alter miRNA biogenesis (Leung and Sharp, 2010). p53 is known to enhance the expression of transcription of certain primary transcripts under DNA damage (Hermeking, 2007) and to associate with p68 to modulate the processing of a restricted population of pri-miRNAs (Suzuki et al., 2009). However, signals and pathways which directly modulate Drosha under either stress or non-stress conditions remain to be identified.

Both miRNAs and proteins involved in miRNA biogenesis are implicated in cell survival and death at various levels. Depending on their specific targets, individual miRNAs can either positively or negatively affect the survival or death process (Afanasyeva et al., 2011; Chong et al., 2010; Formosa et al., 2013; Jovanovic and Hengartner, 2006). There is evidence that the miRNA biogenesis machinery may also have a role in these cellular processes. Interestingly, Dicer seems to play a dual role in regulating cell viability. It is shown to promote survival in diverse types of cells or organisms (Kim et al., 2010; McLoughlin et al., 2012; Mori et al., 2012; Pang et al., 2014; Zehir et al., 2010). However, Drosha also participates in death by cleaving chromosome DNA (Nakagawa et al., 2010). Several studies have hinted that Drosha is involved in either survival or apoptosis (Fan et al., 2013; Han et al., 2013; Vaksman et al., 2012). However, it remains to be clarified how a total of loss of Drosha may impact viability.

RESULTS

Phosphorylation of Drosha by p38 MAPK in response to stress

Since the primary sequence of Drosha contains several proline-directed serine and threonine residues matching the putative phosphorylation sites for MAPK (Figure S1A) (Trempolec et al., 2013), we investigated the possibility that p38 MAPK may directly phosphorylate Drosha. We first tested a direct association of p38 MAPK and Drosha by incubating purified GST-Drosha 210-390aa, which encompasses the RS rich region, with purified active p38 MAPK. This analysis showed that GST-Drosha but not GST specifically pulls down p38 MAPK *in vitro* (Figure S1B). We then used time-resolved fluorescence energy transfer (TR-FRET) to verify the direct association between p38 MAPK and full length Drosha in cellular lysates. This analysis revealed that co-expression of GST-p38 MAPK and its activator MKK3 (mitogen-activated protein kinase kinase 3) with Drosha results in a robust TR-FRET signal (Figure 1A) while GST alone or with MKK3 did not increase TR-FRET over background (Figure S1C), indicating a close proximity of p38 and Drosha typical for proteins which directly associate with each other. To test phosphorylation of Drosha by p38 MAPK, we immunoprecipitated endogenous Drosha from HEK293T cells overexpressing p38 MAPK, and blotted the precipitates with an antibody that specifically recognizes proline-directed phosphorylated serine. This analysis showed that increased p38 MAPK activity leads to Drosha phosphorylation (Figure 1B), which was clearly reduced by p38 inhibitor SB203580. To show that endogenous p38 can mediate this process, we exposed cells to heat or H_2O_2, which induced a rapid increase in p38 MAPK phosphorylation at T180/Y182 (Figure S1D) (Zarubin and Han, 2005), and showed that heat treatment causes a time-dependent increase in phospho Ser signal migrating at Drosha position (Figure 1C, top panel). We knocked down p38 MAPK by siRNA, immunoprecipitated Drosha, and showed that knocking down p38 MAPK significantly attenuates heat-induced phosphorylation of Drosha at its Ser residues (Figure 1C, middle and bottom panels). Similarly, H_2O_2 stress also induced p38-dependent phosphorylation of Drosha (Figure 1D). Together, they indicate that multiple stress signals induce serine phosphorylation of endogenous Drosha via p38 MAPK. To map the phosphorylation sites in Drosha, we over-expressed full length and deletion mutants of Drosha-FLAG in HEK293T cells. Over-expression of full length Drosha generated multiple bands, named a-d (Figure 1E top panel), consistent with the reported detection of multi species of endogenous Drosha protein (Gregory et al., 2004). We used three antibodies which recognize Drosha at its N' terminal region, C' terminal region, and C' terminal FLAG tag to characterize these Drosha bands. Their patterns of recognization indicated that band a represents full length Drosha, band b is truncated at the N' terminus and .bands c and d are truncated at both N' and C' termini. Incubation of the precipitated full length Drosha with purified active p38 MAPK led to a robust phosphorylation of Drosha bands a and b (Figure 1E bottom panels). Since Drosha ΔN220 but not ΔN390 was phosphorylated by p38 MAPK *in vitro*, these results suggested that the region between amino acid residues 220 and 390, which encompasses the RS-rich domain (Figure S1A), should harbor p38 MAPK phosphorylation sites. We purified GST-Drosha 210-390aa and performed *in vitro* p38 kinase assay. p38 MAPK phosphorylated GST-Drosha 210-390aa but not GST (Figure 1F and S1E). Although mutating several of the putative p38 phosphorylation sites individually did not significantly alter the level of phosphorylation of

GST-Drosha 210-390aa (Figure S1F), compound mutants were phosphorylated at a much reduced level. Drosha with five putative p38 sites (S220, S255, T274, S300, and S355) mutated to alanine (mt5) was largely unphosphorylated (Figure 1F). Similar to *in vitro* kinase findings with purified GST-Drosha 201-390aa, mutation of the same five sites also significantly reduced the phosphorylation of either full length Drosha or 1-390aa fragment immunoprecipitated from HEK293T cells, respectively (Figure 1G and S1G). Furthermore, LC-MS/MS analysis of purified GST-Drosha 210-390aa showed that presence of p38 MAPK leads to direct phosphorylation of peptide aa340-360. MS/MS fragment ion information for the phosphorylated peptide spectrum did not allow unambiguous discrimination between Ser355 and Ser357 as the exact site of p38 MAPK directed phosphorylation. Since only Ser355 but not Ser357 is flanked by a proline residue and p38 is a well known proline-directed kinase, it is highly likely that Ser355 is the direct site of p38 phosphorylation (Figure S1H). This is consistent with previous proteomic studies reporting Ser355 phosphorylation (Zhou et al., 2013). To confirm phosphorylation of these sites by p38 MAPK in cells, we immunoprecipitated Drosha-FLAG with the anti-Drosha C' terminal antibody from HEK293 cells and determined Drosha phosphorylation using the phosphoserine antibody. Our results showed that co-expression of p38 MAPK and its activator MKK6 increases Drosha phosphorylation (Figure 1H). Mutation of the five p38 phosphorylation sites significantly reduced its phosphorylation by p38 MAPK. To test whether stress signal can induce Drosha phosphorylation at these sites in cells, we treated the cells briefly with heat or a moderate dose of H_2O_2 (Xia et al., 1995). These led to a robust increase in phosphorylation of wt Drosha (Figure 1I. Full phospho Ser substrate blots for Figure 1 are in Figure S1I). However, heat and H_2O_2 failed to increase phosphorylation of mt5 Drosha. Together, these data indicate that p38 MAPK directly phosphorylates Drosha at multiple sites within its RS-domain in cells in response to cellular stress.

Stress-induced disruption of Drosha and DGCR8 interaction

p38 MAPK is known to translocate into the nucleus in response to cellular stresses (Zarubin and Han, 2005). Drosha stability and its functions to control miRNA biogenesis are modulated by DGCR8 (DiGeorge syndrome critical region 8), its key partner in the microprocessor complex (Han et al., 2009). Stress by heat and H_2O_2 did not reduce the levels of DGCR8 (Figure 2A). Instead, heat and H_2O_2 stress clearly reduced the binding between endogenous Drosha and DGCR8 assessed by co-immunoprecipitation (Figure 2B). Inhibition of p38 by SB203580 or kinase dead p38 (AF) restored the interaction between endogenous Drosha and DGCR8, suggesting that p38 may modulate Drosha-DGCR8 interaction. Consistent with this, over-expression of wt but not kinase dead (AF) p38 with MKK6 in HEK293T cells reduced the binding between endogenous Drosha and DGCR8 (Figure 2C). Activation of p38 also reduced the interaction of GST-DGCR8 with Drosha in a pull-down assay (Figure S2). To show that phosphorylation of Drosha regulates its interaction with DGCR8, we expressed wt or mt5 Drosha-FLAG with or without p38/MKK6 in HEK293T cells, pulled down Drosha with GST-DGCR8, blotted for bound Drosha (Figure 2D, top panel), or alternatively, immunoprecipitated Drosha, and measured bound endogenous DGCR8 (Figure 2D, bottom panel). Both assays showed that co-expression of p38/MKK6 reduce the interaction between wt Drosha and DGCR8 but not between mt5

Drosha and DGCR8. Thus, phosphorylation of Drosha by p38 MAPK reduces its binding to DGCR8.

Stress-induced nuclear export of Drosha

We tested the effect of reduced binding to DGCR8 on the subcellular distribution of endogenous Drosha following stress. Heat and H_2O_2 stress caused a time-dependent decrease in the levels of nuclear Drosha, which correlated with an initial increase in cytoplasmic Drosha (Figure 3A left and middle panels). Our fractionation method yielded relatively clean cytoplasmic and nuclear fractions (Figure 3A right panel and Figure S3A), suggesting that stress changes Drosha subcellular localization. This translocation was not due to a non-specific damage to the nucleus since the levels of DGCR8 and DDX17, nuclear factors known to be associated with Drosha (Kawahara and Mieda-Sato, 2012; Suzuki et al., 2009), did not decrease after either heat or H_2O_2 stress (Figure 3A and S3B). Consistently, immuno cytochemistry analysis also revealed a loss of nuclear Drosha signal following stress (Figure 3B). Prolonged stress eventually led to a reduction of cytoplasmic Drosha. We carried out stress treatment in the presence of SB203580 and showed that similar to inhibition of nuclear exporter CRM1 function with leptomycin B, p38 MAPK inhibitor significantly attenuates stress-induced redistribution of Drosha (Figure 3C). To determine whether translocated Drosha is phosphorylated, we exposed cells to either heat or H_2O_2 for 15 min and measured the levels of Drosha phosphorylated Ser. We confirmed that stress-induced phosphor Ser signal at Drosha position is Drosha since knocking it down completely abolished this phospho signal in whole cell lysates (Figure 3D). Using this approach, we showed that brief stress, while causing either a small increase or no change of the phosphorylated Drosha in the nucleus, leads to a significant elevation in the levels of the phosphorylated Drosha in the cytoplasm (Figure 3E). This change was due to nuclear to cytoplasmic translocation of phosphorylated Drosha since either SB203580 or leptomycin B clearly reduced stress-induced increase of phosphorylated Drosha in the cytoplasm. Together, they indicate that the cytoplasmic translocation of Drosha depends on the p38-mediated phosphorylation.

Stress-induced phosphorylation dependent degradation of Drosha

Prolonged stress eventually resulted in a total reduction of Drosha (Figure 4A). To assess the role of p38 in this, we inhibited p38 MAPK by either SB203580 or p38 (AF) in HEK293 cells and tested their effects on heat- or H_2O_2-induced decrease of Drosha. Inhibition of p38 MAPK significantly protected Drosha from stress-induced reduction (Figure 4B). To determine the role of phosphorylation in Drosha stability, we compared the levels of wt and mt5 Drosha after stress. Prolonged activation of p38 MAPK by co-expression of p38 MAPK and MKK6 clearly reduced the levels of Drosha. This reduction required p38 MAPK activity since inhibitor SB203580 prevented wt Drosha from degradation (Figure 4C). In contrast, mt5 Drosha was much more resistant to p38-mediated degradation (Figure 4D). Similarly, heat and H_2O_2 stress reduced the level of wt Drosha. But the levels of mt5 Drosha and ΔN390 were less sensitive to heat- or H_2O_2-induced degradation (Figure 4E). To strengthen the discoveries, we carried out similar experiments in rat primary cortical neurons and showed that heat and H_2O_2 also induce p38-dependent phosphorylation of Drosha,

reduce its binding to DGCR8, and cause Drosha degradation in neuronal cells (Figure S4), suggesting that stress destabilizes Drosha in multiple types of cells.

Stress-induced cleavage of Drosha by calpain

One of the key proteases activated by stress is calpain (Storr et al., 2011). To test its role in Drosha degradation, we exposed cells with a cell permeable calpain inhibitor calpeptin before H_2O_2 or heat treatment. While H_2O_2 and heat reduced the levels of endogenous Drosha, calpeptin largely protected it from stress-induced degradation (Figure 5A). To establish a direct cleavage of Drosha by calpain, we immunoprecipitated full length or truncated Drosha from cells and incubated the precipitates with purified calpain II in a cleavage assay. Calpain II cleaved full length and ΔN220 Drosha. This could be blocked by calpeptin (Figure 5B). In contrast, ΔN390 was much more resistant to the cleavage by calpain *in vitro*. To analyze the effects of phosphorylation on Drosha cleavage, we expressed Drosha in HEK293T cells with or without p38/MKK6, immunoprecipitated comparable amounts of Drosha, and subjected the precipitates to calpain cleavage at 0°C. This milder cleavage condition revealed that Drosha is more resistant to degradation by calpain in the absence of p38/MKK6 co-expression (Figure 5B bottom panels). Interestingly, cleavage of full length Drosha was accompanied by the appearance of a smaller cleaved fragment (Figure 5B bottom right). Exposure of HEK293 cells to stress also led to the generation of a small cleaved fragment with the same size. Importantly, its generation required the activities of cellular calpain and p38 MAPK (Figure 5C). Thus, calpain cleaves phosphorylated Drosha to facilitate stress-induced degradation.

Inhibition of miRNA biogenesis by stress-induced regulaton of Drosha

The known primary cellular function of Drosha is to regulate miRNA biogenesis (Kim, 2005). We tested the effect of heat on pre-miRNA biogenesis since heat stress causes a more acute and synchronized change in Drosha. We prepared small RNA/miRNA by PureLink Isolation Kit because gel electrophoresis and quantitative real time PCR (qRT-PCR) analysis indicated that this small RNA sample contains pre-miRNAs but not large RNAs compared to RNA sample prepared by TRIzol (Figure S5A). Analysis of the selected endogenous pre-miRNAs by qRT-PCR showed that heat stress significantly reduces the levels of all the endogenous pre-miRNAs tested (Figure 6A left panel). SB203580 largely reversed the effect of heat. The decrease in pre-miRNA was unlikely caused by heat-induced non-specific reduction of pri-miRNA because compared to unheated controls; the levels of pri-miRNAs in the RNA samples isolated by TRIzol were unchanged, reduced, or increased after heat (Figure 6A right panel and Figure S5B). Consistent with qRT-PCR results, analysis of small RNA samples by Northern blot showed that heat stress reduces the levels of endogenous pre- and mature miRNAs tested (Figure 6B). To confirm this inhibitory effect on pre-miRNAs is mediated through Drosha, we immunoprecipitated Drosha following expression in HEK293T cells, incubated with an internally labeled model substrate pri-miR-30a in a processing assay, measured the generation of pre-miR-30a by autoradiograph (Lee and Kim, 2007). Incubation of the model pri-miR-30a with Drosha led to the conversion of the large pri-to pre-miR-30a compared to controls (Figure 6C left panel). Co-expression of p38 MAPK with Drosha significantly reduced this conversion while SB203580 restored the level of pre-miR-30a (Figure 6C right panel). To corroborate the *in vitro* conversion findings, we

measured the levels of model pre-miR-30a generated in cells by Drosha using Northern blot assay. Over-expression of Drosha significantly increased the premiR-30a level. Co-expression of p38 MAPK/MKK6 largely blocked the increase in pre-miR-30a level. SB203580 restored the efficiency of Drosha-mediated conversion (Figure 6D left panel). Similarly, heat treatment also reduced the level of model pre-miR-30a while SB203580 restored it (Figure 6D right panel). To show that phosphorylation of Drosha is involved, we expressed wt or mt5 Drosha, treated cells with heat or H2O2, and tested the immunoprecipitated Drosha in pre-miR30a conversion assay. This analysis showed that heat and H_2O_2 effectively reduce wt Drosha-mediated conversion but the conversion mediated by mt5 Drosha was largely insensitive to the inhibitory effect of stress (Figure 6E and S5C). Thus, phosphorylation by p38 MAPK following stress reduces Drosha-mediated pre-miRNA biogenesis.

Regulation of Drosha-mediated survival by stress

Since prolonged and severe cellular stress activates p38 MAPK and causes cell death, we investigated the role of Drosha in stress-induced death. Under our experimental condition, H_2O_2 robustly activated p38 MAPK (Figure S1D) and induced a p38 MAPK-dependent death of HEK293T cells (Figure S6). Time course analysis showed that H_2O_2-induced time dependent decrease of Drosha clearly precedes the activation of caspase 3 (Figure 7A), suggesting that loss of Drosha may play a role in H_2O_2-induced death. To test this, we over-expressed different amounts of Drosha in HEK293T cells (Figure 7B bottom panel) and treated cells with various concentrations of H_2O_2. Viability measurement indicated that levels of Drosha correlate closely with their viability under H_2O_2-induced stress (Figure 7B top panel). In converse experiments, we knocked down Drosha and showed that this sensitizes cells to H_2O_2-induced stress (Figure 7C). Consistent with these findings, increasing Drosha level attenuated H_2O_2-induced activation of caspase 3 measured in live cells using a fluorescent substrate (Figure 7D top panel) or by immunoblotting (Figure 7E top panel). Conversely, knockdown of Drosha increased the levels of activated caspase 3 following H_2O_2 (Figure 7D and 7E, bottom panels). Moreover, compared to wt Drosha, cells expressing mt5 Drosha had higher levels of survival under H_2O_2 (Figure 7F). Thus, Drosha protects cells from H_2O_2-induced apoptosis.

DISCUSSION

Production of miRNA production is a highly controlled process. Increasing evidence indicates that miRNA biogenic associated proteins are regulated (Han et al., 2009; Heo and Kim, 2009). Drosha is thought to reside in two types of complexes (Gregory et al., 2004), one composed of solely Drosha and DGCR8 and the other of additional accessory proteins including DEAD-box helicases p68 and p72. Recent studies showed that pri-miRNA processing is modulated by TGFβ/BMP-SMADs (Davis et al., 2010), DNA damage/p53 (Suzuki et al., 2009), estrogen/estrogen receptor alpha (Suzuki et al., 2009), and MeCP2 (Cheng et al., 2014). In these examples, regulatory signals converge their activities on accessory proteins such as p68 or DGCR8 but not Drosha (Newman and Hammond, 2010). Although Drosha has been shown to be phosphorylated *in vitro* by glycogen synthase kinase 3 beta (GSK3β) (Tang et al., 2011), its upstream signal or significance is unclear. Therefore,

our findings here provide the first example of signal-mediated direct phosphorylation and regulation of Drosha in a biological process.

Emerging studies suggest that stress can alter miRNA biogenesis (Leung and Sharp, 2010). Our study revealed a direct and tight control of Drosha by stress conditions and an unexpected critical role of this regulation in cell survival. Drosha appears to be both necessary and sufficient for cell survival. Phosphorylation-mediated degradation of Drosha underlies in part stress-induced cell death. How Drosha promotes cell survival under stress is currently not clear. One possible mechanism is through its miRNA biogenic function. Several examples have demonstrated that loss of individual miRNA may render model animals vulnerable in stress conditions (Flynt et al., 2009; Li et al., 2009; van Rooij et al., 2007; Xu et al., 2003). Since stress-induced phosphorylation and degradation of Drosha is accompanied closely by an overall loss of pri-miRNA processing activity, this is consistent with the idea that a global reduction in miRNAs sensitizes cells to stress (Ambros, 2003; Brennecke et al., 2003). However, our data do not exclude the possibility that Drosha may function in part independent of its role in miRNA biogenesis to promote cell survival. In support of this possibility, it should be noted that absence of Drosha or Dicer does not always produce the same effects (Babiarz et al., 2008; Chong et al., 2010; Oskowitz et al., 2011) and Drosha has been reported to regulate neurogenesis independent of miRNAs (Knuckles et al., 2012). Further studies are needed to clarify this issue.

A previous study found that DGCR8 stabilizes Drosha via protein-protein interaction. But how this interaction stabilizes Drosha and whether it is regulated are not clear (Han et al., 2004). Our study suggests that this interaction is highly sensitive to stress and negatively controlled by p38 MAPK-mediated phosphorylation of Drosha. How phosphorylation of Drosha by p38 MAPK reduces its interaction with DGCR8 is not clear. One possibility is that phosphorylation at multiple sites in the highly charged RS-rich region alter Drohsa confirmation, which in turn weakens its binding to DGCR8. Loss of this interaction upon stress subjects Drosha to nuclear export and subsequent cleavage by calpain. The presence of multiple bands of Drosha suggests that the protein is highly processed and regulation of its stability is likely complex. Some degree of degradation of Drosha may occur under condition when no overt additional stress is applied. It is very possible that degradation of Drosha under basal condition is very inefficient and stress-induced phosphorylation greatly enhances it. Although p38 MAPK and calpain both are key mediators of cellular stress (Lee et al., 2000; Su et al., 2010), they are also activated in response to non-stress signals or under non-pathological conditions to regulate a variety of cellular processes. In support of this, p38 downstream effector kinase MK2 has recently been shown to modulate the localization of argonaute 2 to processing bodies and of microprocessor component p68 in the nucleus under cellular growth conditions (Hong et al., 2013; Zeng et al., 2008). Together, these results indicate that p38 MAPK is capable of mediating both stress and non-stress signals to directly or indirectly modulate Drosha function to either impair or enhance miRNA biogenesis.

Our findings suggest that phosphorylation of Drosha at multiple sites including S300 promotes its translocation to the cytoplasm. Interestingly, GSK3β can phosphorylate Drosha at S300 and S302 *in vitro*. This has been reported to promote the nuclear localization of

Drosha under basal condition (Tang et al., 2011). Thus, it appears that phosphorylation of S300 by GSK3β and p38 MAPK is involved in opposing processes. The reason for this is not clear. It is possible that the extensive phosphorylation induced by stress over a much wide region at the N terminal RS-rich domain of Drosha may mask or override the nuclear localization function resulting from the more discrete phosphorylation at S300 and S302. Together, they further suggest that modulating Drosha subcellular localization is an important mechanism in regulation of Drosha.

EXPERIMENTAL PROCEDURES

Plasmids and antibody

pCMV-miR-30a was purchased from Origene. Anti-N'-Drosha antibody was purchased from Abcam (ab12286), and antibodies to phospho S/P (2325), phospho p38 (9211), C'-Drosha (3364s), and cleaved caspase 3 (9664) from Cell Signaling (9542).

Time-resolved fluorescence resonance energy transfer (TR-FRET) assay

Procedures for TR-FRET assay were the same as previously described (Du et al., 2013; Du and Havel, 2012). Briefly, overexpressed proteins (Drosha-FLAG, FLAG-MKK3, GST-p38 and GST-MKK3) from various cell lysates after transfection were collected and diluted in FRET buffer. FRET detection antibody mixture containing anti-FLAG-Terbium and anti-GST-D2 diluted in FRET buffer was added to the lysates. After incubation (4° for 16 h), the TR-FRET signal was detected using Envision Multilabel plate reader with the laser excitation at 337 nm and emission 1 at 615 nm and emission 2 at 665 nm.

In vitro kinase assay

Purified Drosha-FLAG or Drosha-FLAG fragment recombinant proteins were incubated with active p38α (EMD) in a kinase buffer (containing 20 μM ATP and 10 μCi of γ-^{32}P-ATP for 30 min at 30°C.

In vitro digestion assay

Immunoprecipitated Drosha-FLAG was incubated with Calpain II (EMD) in digestion buffer (50 mM Tris-HCl pH 7.4, 1 mM $CaCl_2$, and 2 mM DTT) on ice for the indicated period of time.

In vitro pri-miRNA processing assay

Cellular extracts or purified Drosha-FLAG were mixed with processing assay buffer (6.4 mM $MgCl_2$, 3 μl 10^4-10^5 cpm of radiolabled pri-miRNA-30a, and 1U RNase inhibitor). The reaction mixture was incubated at 37°C for 90 min. The RNA was extracted and separated on denaturing 15% polyacrylamide gel.

qRT-PCR assay

Total RNA or small RNA was isolated using TRIzol or PureLink miRNA isolation Kit. cDNA was synthesized from 1 μg of purified RNA by SuperScript II First-Strand cDNA synthesis system (Invitrogen). Primer sequences for qRT-PCR were described by Suzuki et

al (Suzuki et al., 2009). Primer pairs for each pre-miRNA were designed with the forward primer being within its mature miR-5p and the reverse one being within its mature miR-3p sequences with a maximal extension of 4 nt except for pre-miR-21 primers, which extended 7 nt outside of the mature miR-21 sequence. qRT-PCR was performed with SYBR Green Brilliant III Ultral-fast reagent kit (MX3000P, Stratagene). The results of qRT-PCR assays presented are an average of three independent RNA preparations. Each sample was analyzed in triplicates.

Northern blot assay

RNA samples isolated using PureLink miRNA isolation Kit (Ambion, K1570-01) or TRIzol were separated on denaturing 15% polyacrylamide gel and probed with Highly Sensitive MiRNA Northern Blot Kit (Signosis, #NB-1001) or 5'-^{32}P-phosphorylated DNA oligo probe, respectively.

Cell viability and survival assay

Cells were transfected with plasmids or RNA for 24 h, treated with H_2O_2 for the indicated periods of time, and incubated with 50 μl of WST-1 solution for 2 h in 24 well plates. Cell viability was measured at 450 nm in microplate reader. Live cell caspase-3 detection assay was performed by using NucView488 Caspase-3 detection kit as instructed (Biotium) (Cen et al., 2008).

Statistical analysis

The results were repeated at least three experiments. Statistical analyses were performed by the Analysis of Variance (ANOVA) with corresponding post hoc tests. Differences were accepted as significant at $p<0.05$.

Supplementary Material

Refer to Web version on PubMed Central for supplementary material.

ACKNOWLEDGMENTS

We thank Dr. V. Narry Kim for Drosha and DGCR8 constructs. This work was in part supported by grants to Z.M (NIH AG023695, NS079858, and ES015317), to Q.Y (National Natural Science Foundation of China 31371400 and Chinese National 973 Project 2011CB510000) and to the Emory Neuroscience NINDS Core Facilities P30 (NS055077), and by the Emory Chemical Biology Discovery Center (Y.D and H.F).

References

Afanasyeva EA, Mestdagh P, Kumps C, Vandesompele J, Ehemann V, Theissen J, Fischer M, Zapatka M, Brors B, Savelyeva L, et al. MicroRNA miR-885-5p targets CDK2 and MCM5, activates p53 and inhibits proliferation and survival. Cell death and differentiation. 2011; 18:974–984. [PubMed: 21233845]

Ambros V. MicroRNA pathways in flies and worms: growth, death, fat, stress, and timing. Cell. 2003; 113:673–676. [PubMed: 12809598]

Babiarz JE, Ruby JG, Wang Y, Bartel DP, Blelloch R. Mouse ES cells express endogenous shRNAs, siRNAs, and other Microprocessor-independent, Dicer-dependent small RNAs. Genes Dev. 2008; 22:2773–2785. [PubMed: 18923076]

Brennecke J, Hipfner DR, Stark A, Russell RB, Cohen SM. bantam encodes a developmentally regulated microRNA that controls cell proliferation and regulates the proapoptotic gene hid in Drosophila. Cell. 2003; 113:25–36. [PubMed: 12679032]

Cen H, Mao F, Aronchik I, Fuentes RJ, Firestone GL. DEVD NucView488: a novel class of enzyme substrates for real-time detection of caspase-3 activity in live cells. The FASEB journal : official publication of the Federation of American Societies for Experimental Biology. 2008; 22:2243–2252. [PubMed: 18263700]

Cheng TL, Wang Z, Liao Q, Zhu Y, Zhou WH, Xu W, Qiu Z. MeCP2 suppresses nuclear microRNA processing and dendritic growth by regulating the DGCR8/Drosha complex. Developmental cell. 2014; 28:547–560. [PubMed: 24636259]

Chong MM, Zhang G, Cheloufi S, Neubert TA, Hannon GJ, Littman DR. Canonical and alternate functions of the microRNA biogenesis machinery. Genes Dev. 2010; 24:1951–1960. [PubMed: 20713509]

Davis BN, Hilyard AC, Nguyen PH, Lagna G, Hata A. Smad proteins bind a conserved RNA sequence to promote microRNA maturation by Drosha. Molecular cell. 2010; 39:373–384. [PubMed: 20705240]

Du Y, Fu RW, Lou B, Zhao J, Qui M, Khuri FR, Fu H. A time-resolved fluorescence resonance energy transfer assay for high-throughput screening of 14-3-3 protein-protein interaction inhibitors. Assay and drug development technologies. 2013; 11:367–381. [PubMed: 23906346]

Du YH, Havel JJ. Time-Resolved Fluorescence Resonance Energy Transfer Technologies in HTS. Chemical Genomics. 2012:198–214.

Fan P, Chen Z, Tian P, Liu W, Jiao Y, Xue Y, Bhattacharya A, Wu J, Lu M, Guo Y, et al. miRNA biogenesis enzyme Drosha is required for vascular smooth muscle cell survival. PloS one. 2013; 8:e60888. [PubMed: 23637774]

Flynt AS, Thatcher EJ, Burkewitz K, Li N, Liu Y, Patton JG. miR-8 microRNAs regulate the response to osmotic stress in zebrafish embryos. The Journal of cell biology. 2009; 185:115–127. [PubMed: 19332888]

Formosa A, Markert EK, Lena AM, Italiano D, Finazzi-Agro E, Levine AJ, Bernardini S, Garabadgiu AV, Melino G, Candi E. MicroRNAs, miR-154, miR-299-5p, miR-376a, miR-376c, miR-377, miR-381, miR-487b, miR-485-3p, miR-495 and miR-654-3p, mapped to the 14q32.31 locus, regulate proliferation, apoptosis, migration and invasion in metastatic prostate cancer cells. Oncogene. 2013

Gregory RI, Yan KP, Amuthan G, Chendrimada T, Doratotaj B, Cooch N, Shiekhattar R. The Microprocessor complex mediates the genesis of microRNAs. Nature. 2004; 432:235–240. [PubMed: 15531877]

Han J, Lee Y, Yeom KH, Kim YK, Jin H, Kim VN. The Drosha-DGCR8 complex in primary microRNA processing. Genes Dev. 2004; 18:3016–3027. [PubMed: 15574589]

Han J, Pedersen JS, Kwon SC, Belair CD, Kim YK, Yeom KH, Yang WY, Haussler D, Blelloch R, Kim VN. Posttranscriptional crossregulation between Drosha and DGCR8. Cell. 2009; 136:75–84. [PubMed: 19135890]

Han Y, Liu Y, Gui Y, Cai Z. Inducing cell proliferation inhibition and apoptosis via silencing Dicer, Drosha, and Exportin 5 in urothelial carcinoma of the bladder. Journal of surgical oncology. 2013; 107:201–205. [PubMed: 22766726]

Heo I, Kim VN. Regulating the regulators: posttranslational modifications of RNA silencing factors. Cell. 2009; 139:28–31. [PubMed: 19804751]

Herbert KM, Pimienta G, DeGregorio SJ, Alexandrov A, Steitz JA. Phosphorylation of DGCR8 increases its intracellular stability and induces a progrowth miRNA profile. Cell reports. 2013; 5:1070–1081. [PubMed: 24239349]

Hermeking H. p53 enters the microRNA world. Cancer cell. 2007; 12:414–418. [PubMed: 17996645]

Hong S, Noh H, Chen H, Padia R, Pan ZK, Su SB, Jing Q, Ding HF, Huang S. Signaling by p38 MAPK stimulates nuclear localization of the microprocessor component p68 for processing of selected primary microRNAs. Science signaling. 2013; 6:ra16. [PubMed: 23482664]

Jovanovic M, Hengartner MO. miRNAs and apoptosis: RNAs to die for. Oncogene. 2006; 25:6176–6187. [PubMed: 17028597]

Kawahara Y, Mieda-Sato A. TDP-43 promotes microRNA biogenesis as a component of the Drosha and Dicer complexes. Proceedings of the National Academy of Sciences of the United States of America. 2012; 109:3347–3352. [PubMed: 22323604]

Kim GJ, Georg I, Scherthan H, Merkenschlager M, Guillou F, Scherer G, Barrionuevo F. Dicer is required for Sertoli cell function and survival. The International journal of developmental biology. 2010; 54:867–875. [PubMed: 19876815]

Kim VN. MicroRNA biogenesis: coordinated cropping and dicing. Nature reviews. Molecular cell biology. 2005; 6:376–385. [PubMed: 15852042]

Knuckles P, Vogt MA, Lugert S, Milo M, Chong MM, Hautbergue GM, Wilson SA, Littman DR, Taylor V. Drosha regulates neurogenesis by controlling neurogenin 2 expression independent of microRNAs. Nature neuroscience. 2012; 15:962–969. [PubMed: 22706270]

Lee MS, Kwon YT, Li M, Peng J, Friedlander RM, Tsai LH. Neurotoxicity induces cleavage of p35 to p25 by calpain. Nature. 2000; 405:360–364. [PubMed: 10830966]

Lee RC, Feinbaum RL, Ambros V. The C. elegans heterochronic gene lin-4 encodes small RNAs with antisense complementarity to lin-14. Cell. 1993; 75:843–854. [PubMed: 8252621]

Lee Y, Ahn C, Han J, Choi H, Kim J, Yim J, Lee J, Provost P, Radmark O, Kim S, et al. The nuclear RNase III Drosha initiates microRNA processing. Nature. 2003; 425:415–419. [PubMed: 14508493]

Lee Y, Kim VN. In vitro and in vivo assays for the activity of Drosha complex. Methods in enzymology. 2007; 427:89–106. [PubMed: 17720480]

Leung AK, Sharp PA. MicroRNA functions in stress responses. Molecular cell. 2010; 40:205–215. [PubMed: 20965416]

Li X, Cassidy JJ, Reinke CA, Fischboeck S, Carthew RW. A microRNA imparts robustness against environmental fluctuation during development. Cell. 2009; 137:273–282. [PubMed: 19379693]

McLoughlin HS, Fineberg SK, Ghosh LL, Tecedor L, Davidson BL. Dicer is required for proliferation, viability, migration and differentiation in corticoneurogenesis. Neuroscience. 2012; 223:285–295. [PubMed: 22898830]

Michlewski G, Caceres JF. Antagonistic role of hnRNP A1 and KSRP in the regulation of let-7a biogenesis. Nature structural & molecular biology. 2010; 17:1011–1018.

Mori MA, Raghavan P, Thomou T, Boucher J, Robida-Stubbs S, Macotela Y, Russell SJ, Kirkland JL, Blackwell TK, Kahn CR. Role of microRNA processing in adipose tissue in stress defense and longevity. Cell metabolism. 2012; 16:336–347. [PubMed: 22958919]

Nakagawa A, Shi Y, Kage-Nakadai E, Mitani S, Xue D. Caspase-dependent conversion of Dicer ribonuclease into a death-promoting deoxyribonuclease. Science. 2010; 328:327–334. [PubMed: 20223951]

Newman MA, Hammond SM. Emerging paradigms of regulated microRNA processing. Genes Dev. 2010; 24:1086–1092. [PubMed: 20516194]

Oskowitz AZ, Penfornis P, Tucker A, Prockop DJ, Pochampally R. Drosha regulates hMSCs cell cycle progression through a miRNA independent mechanism. Int J Biochem Cell Biol. 2011; 43:1563–1572. [PubMed: 21794839]

Pang X, Hogan EM, Casserly A, Gao G, Gardner PD, Tapper AR. Dicer expression is essential for adult midbrain dopaminergic neuron maintenance and survival. Molecular and cellular neurosciences. 2014; 58:22–28. [PubMed: 24184162]

Paroo Z, Ye X, Chen S, Liu Q. Phosphorylation of the human microRNA-generating complex mediates MAPK/Erk signaling. Cell. 2009; 139:112–122. [PubMed: 19804757]

Shapiro JS, Langlois RA, Pham AM, Tenoever BR. Evidence for a cytoplasmic microprocessor of pri-miRNAs. Rna. 2012; 18:1338–1346. [PubMed: 22635403]

Storr SJ, Carragher NO, Frame MC, Parr T, Martin SG. The calpain system and cancer. Nature reviews. Cancer. 2011; 11:364–374. [PubMed: 21508973]

Su LT, Chen HC, Gonzalez-Pagan O, Overton JD, Xie J, Yue L, Runnels LW. TRPM7 activates m-calpain by stress-dependent stimulation of p38 MAPK and c-Jun N-terminal kinase. Journal of molecular biology. 2010; 396:858–869. [PubMed: 20070945]

Suzuki HI, Yamagata K, Sugimoto K, Iwamoto T, Kato S, Miyazono K. Modulation of microRNA processing by p53. Nature. 2009; 460:529–533. [PubMed: 19626115]

Tang X, Li M, Tucker L, Ramratnam B. Glycogen synthase kinase 3 beta (GSK3beta) phosphorylates the RNAase III enzyme Drosha at S300 and S302. PloS one. 2011; 6:e20391. [PubMed: 21674040]

Trempolec N, Dave-Coll N, Nebreda AR. SnapShot: p38 MAPK substrates. Cell. 2013; 152:924–924. e921. [PubMed: 23415236]

Vaksman O, Hetland TE, Trope CG, Reich R, Davidson B. Argonaute, Dicer, and Drosha are up-regulated along tumor progression in serous ovarian carcinoma. Human pathology. 2012; 43:2062–2069. [PubMed: 22647351]

van Rooij E, Sutherland LB, Qi X, Richardson JA, Hill J, Olson EN. Control of stress-dependent cardiac growth and gene expression by a microRNA. Science. 2007; 316:575–579. [PubMed: 17379774]

Wu H, Sun S, Tu K, Gao Y, Xie B, Krainer AR, Zhu J. A splicing-independent function of SF2/ASF in microRNA processing. Molecular cell. 2010; 38:67–77. [PubMed: 20385090]

Xia Z, Dickens M, Raingeaud J, Davis RJ, Greenberg ME. Opposing effects of ERK and JNK-p38 MAP kinases on apoptosis. Science. 1995; 270:1326–1331. [PubMed: 7481820]

Xu P, Vernooy SY, Guo M, Hay BA. The Drosophila microRNA Mir-14 suppresses cell death and is required for normal fat metabolism. Current biology : CB. 2003; 13:790–795. [PubMed: 12725740]

Zarubin T, Han J. Activation and signaling of the p38 MAP kinase pathway. Cell Res. 2005; 15:11–18. [PubMed: 15686620]

Zehir A, Hua LL, Maska EL, Morikawa Y, Cserjesi P. Dicer is required for survival of differentiating neural crest cells. Developmental biology. 2010; 340:459–467. [PubMed: 20144605]

Zeng Y, Sankala H, Zhang X, Graves PR. Phosphorylation of Argonaute 2 at serine-387 facilitates its localization to processing bodies. The Biochemical journal. 2008; 413:429–436. [PubMed: 18476811]

Zhou H, Di Palma S, Preisinger C, Peng M, Polat AN, Heck AJ, Mohammed S. Toward a comprehensive characterization of a human cancer cell phosphoproteome. Journal of proteome research. 2013; 12:260–271. [PubMed: 23186163]

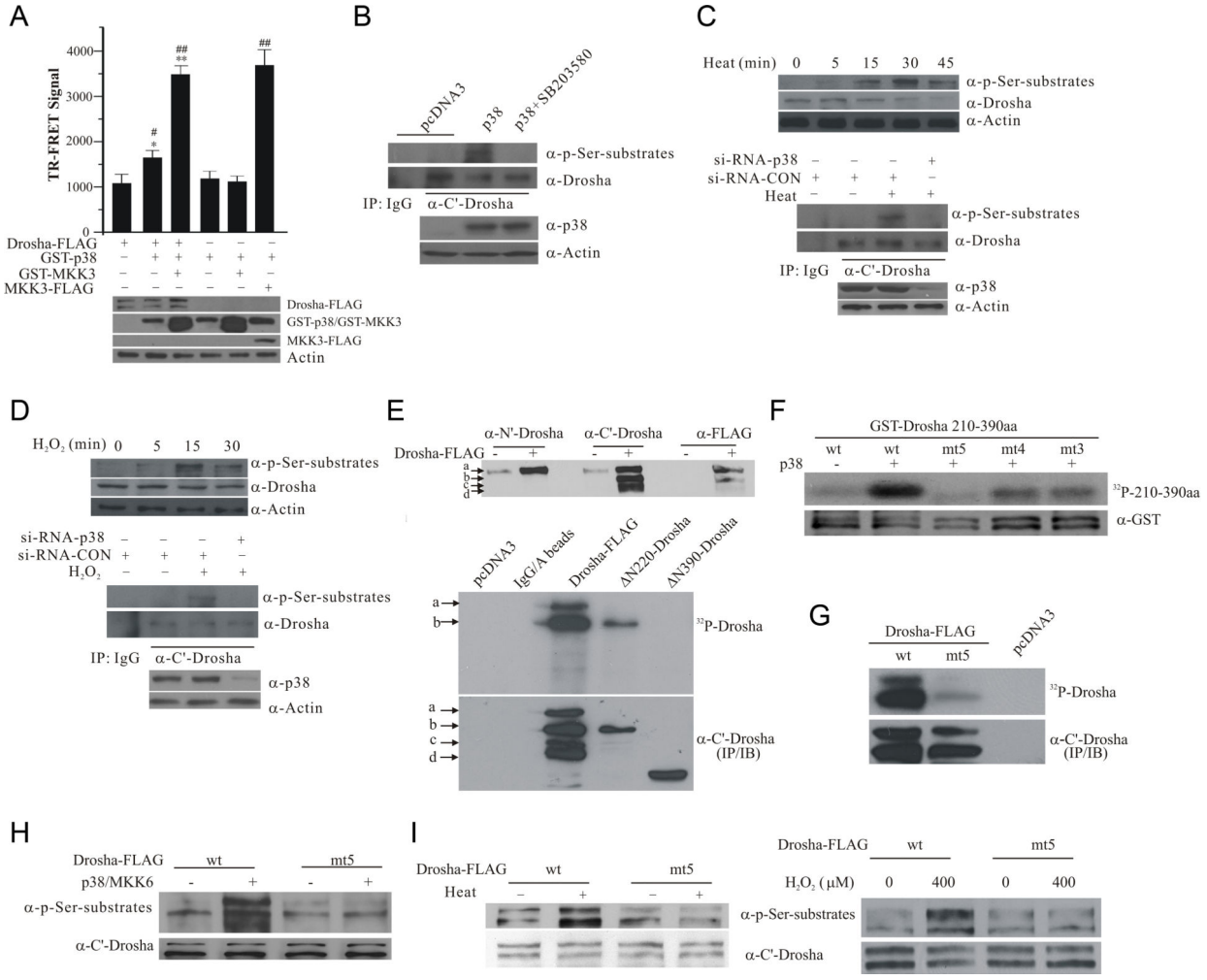

Figure 1.

Phosphorylation of Drosha RS-rich domain by p38 MAPK. (A) Interaction between Drosha and p38 by TR-FRET. HEK293 cells were transfected with various plasmids carrying Drosha-FLAG, FLAG-MKK3, GST-p38 and GST-MKK3. Over-expressed proteins immunoprecipitated from lysates were tested for TR-FRET signal. The top panel shows TR-FRET signal expressed as ratio (A665/A615 × 10^4). The data were expressed as mean ± SD from triplicate samples (*p <0.05 or **p < 0.01 vs Drosha-FLAG alone group and $^{\#}p < 0.05$ or $^{\#\#}p < 0.01$ vs GST-p38 alone group; ANONA with Dunnett's Test). The bottom panel shows the expression of Drosha-FLAG, GST-p38, GST-MKK3, and FLAG-MKK3. **(B)** p38 MAPK-induced phosphorylation of endogenous Drosha. Endogenous Drosha immunoprecipitated from HEK293 cells transfected as indicated was blotted with an anti-phospho Ser followed by a proline (top panel). The bottom panel shows the levels of p38. **(C)** Heat-induced phosphorylation of endogenous Drosha in HEK293 cells. Levels of phosphorylated Drosha in cellular lysates were measured by anti-phospho Ser blotting after heat (45°C) treatment (top panel). Drosha immunoprecipitated from HEK293 cells transfected and treated with heat for 15 min was blotted with anti-phospho Ser antibody (middle and bottom panels). **(D)** H_2O_2-induced phosphorylation of endogenous Drosha in

HEK293 cells. The experiments were carried out as described in (C) with H_2O_2 (400 μM) treatment of various time (top panel) or 15 min. **(E)** Mapping the phosphorylation domain of Drosha by direct p38 kinase assay. Top panel shows multiple species of Drosha-FLAG marked as a-d recognized by the indicated antibodies in HEK293 lysates over-expressing Drosha-FLAG. Middle panel shows the autoradiograph of *in vitro* p38 MAPK kinase reaction with Drosha-FLAG, ΔN220-Drosha-FLAG and ΔN390-Drosha-FLAG immunoprecipitated from HEK293T cells with the anti-C' Drosha antibody. The same membrane was probed by anti-C' terminal Drosha antibody (bottom panel). **(F)** Identification of p38 phosphorylation sites in Drosha RS-rich domain. Purified GST-Drosha 210-390aa was incubated with purified p38 MAPK in kinase assay (top panel, autoradiograph). The same membrane was blotted with an anti-GST antibody (bottom panel) (wild type: wt; mutants: mt3, S220A, S255A, and T274A; mt4, S220A, S255A, T274A, and S300A; and mt5, S220A, S255A, T274A, S300A, and S355A). **(G)** Phosphorylation of Drosha by p38 MAPK. Drosha-FLAG (wt and mt5) was immunoprecipitated from cells with anti-C' terminal Drosha antibody and phosphorylated by p38 MAPK *in vitro*. (**H**) Phosphorylation of Drosha by p38 MAPK in cells. Cell lysates from HEK293T cells transfected as indicated were blotted with the phospho Ser antibody. The same membrane was re-probed with anti-C' Drosha antibody. **(I)** Heat- or H_2O_2-induced phosphorylation of Drosha. HEK293T cells after transfection were treated with heat (45°C) or H_2O_2 (400 μM) for 15 min. Lysates were blotted as described in **(H)**. See also Figure S1.

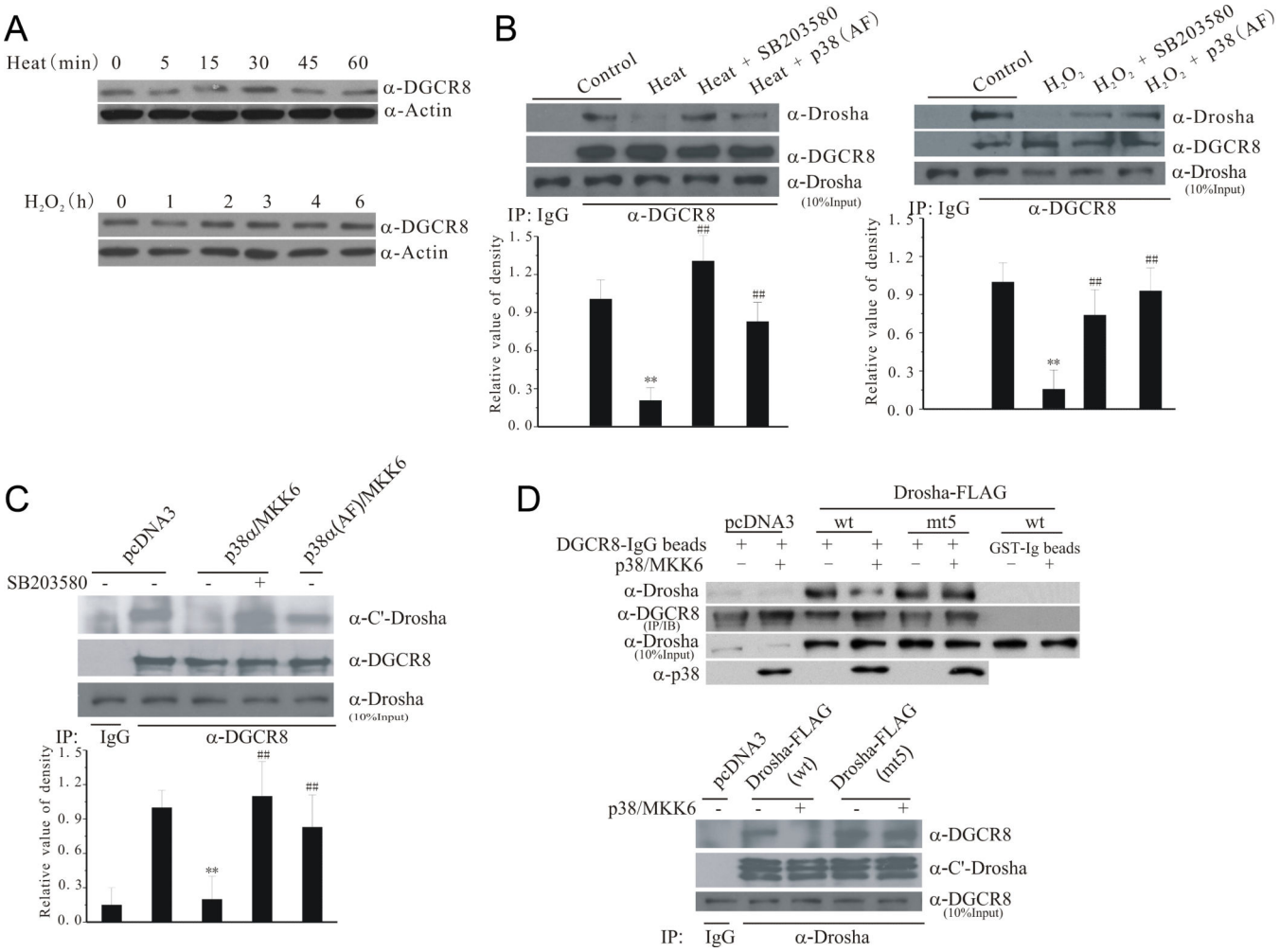

Figure 2.

Stress-induced loss of interaction between Drosha and DGCR8. **(A)** Levels of DGCR8 following stress. Lysates from HEK293 treated with heat (45°C) or H_2O_2 (400 μM) were blotted for DGCR8. **(B)** Stress-induced dissociation of endogenous Drosha and DGCR8 complex. Lysates of HEK293 cells after treatment with heat (15 min) or H_2O_2 (30 min) were immunoprecipitated with an anti-DGCR8 antibody (20 μM SB203580 was added 30 min and p38 (AF) was transfected over-night before treatment). The precipitates were blotted for Drosha. The bottom graphs show the quantification of Drosha levels (mean ± SEM, n = 4, **p < 0.01 vs control; $^{\#\#}$p < 0.01 vs heat or H_2O_2 alone). **(C)** Active p38-induced dissociation of endogenous Drosha and DGCR8 complex. HEK293 cells were transfected for 12 h and treated with SB203580 (20 μM) or vehicle for 16 h. Binding of endogenous Drosha and DGCR8 was assessed by co-IP. The bottom graph shows the quantification of Drosha levels (mean ± SEM, n = 4, **p < 0.01 vs pcDNA3; $^{\#\#}$p < 0.01 vs p38α/MKK6). **(D)** Resistance to p38-induced dissociation by mt5 Drosha. Drosha from the transfected HEK293 cells was pulled down with GST-DGCR8 (top panel) or co-immunoprecipitated as described in (C) (bottom panel). See also Figure S2.

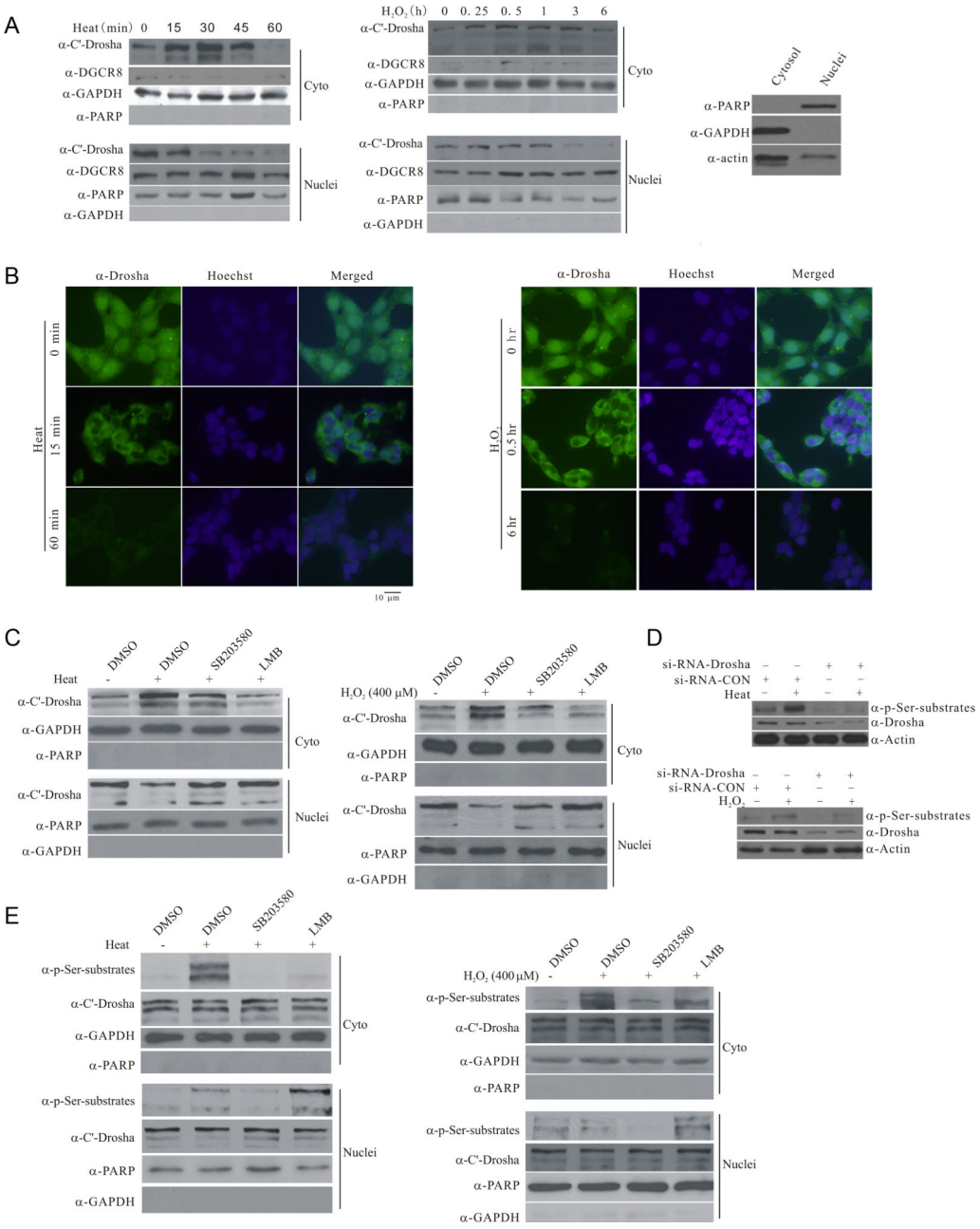

Figure 3.

Stress-induced phosphorylation-dependent nuclear export of Drosha. **(A)** Stress-induced changes in the subcellular distribution of endogenous Drosha. HEK293 cells were exposed to heat (45°C) or H_2O_2 (400 μM) for the indicated time. Cytoplasmic and nuclear fractions were blotted for Drosha, cytoplasmic marker GAPDH or nuclear marker PARP1 (PARP). Right panel shows the cross contamination of cytoplasmic and nuclear fractions yielded by the Sigma Nuclei EZ Prep Kit (Nuc-01). **(B)** Stress-induced changes in the subcellular distribution of endogenous Drosha by immunocytochemistry. HEK297 cells were exposed to heat (45°C) or H_2O_2 (400 μM) for the indicated time. The cells were stained with anti-Drosha antibody or Hoechst33324. All Drosha images were acquired with 200 ms exposure

time and Hoechst image 10 ms exposure time. **(C)** Stress-induced p38 MAPK dependent accumulation of endogenous Drosha in the cytoplasm. HEK293T cells were treated with SB203580 (20 μM) or leptomycin B (LMB, 5 ng/ml) for 30 min and exposed to heat (45°C, 30 min) or H_2O_2 (400 μM, 30 min). The levels of Drosha in the cytoplasmic and nuclear fractions were determined. **(D)** Recognition of stress-induced Drosha phosphorylation by anti-phospho Ser antibody. HEK293 cells were transfected with si-RNA-Drosha or si-RNA-control for 72 h and exposed to heat (45°C) or H_2O_2 (400 μM) for 15 min. The proteins were collected for western blot with anti-phospho Ser antibody. **(E)** Stress-induced nuclear export of phosphorylated Drosha. HEK293 cells were treated as in (C) with 15 min stress. See also Figure S3.

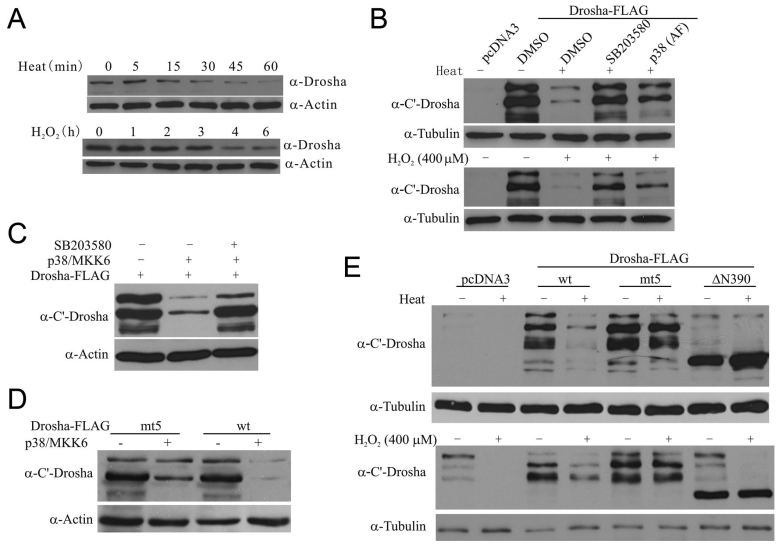

Figure 4.

Stress-induced degradation of Drosha. **(A)** Stress-induced degradation of endogenous Drosha. Lysates from HEK293 cells treated with heat (45°C) or H_2O_2 (400 μM) were blotted for Drosha. **(B)** Effects of inhibiting p38 MAPK on stress-induced degradation of Drosha. HEK293 cells were transfected as indicated and treated with Heat (45°C, 45 min) or H_2O_2 (400 μM, 8 h). SB203580 was added to cells 30 min prior to stress treatment. **(C)** p38-induced decrease in the level of Drosha. HEK293T cells were transfected as indicated for 12 h and treated with SB203580 (20 μM) or vehicle for 16 h. **(D)** Resistance to p38 MAPK-induced degradation by mt5 Drosha-FLAG. Levels of wt and mt5 Drosha in HEK293T cells after transfection were determined. **(E)** Resistance to stress-induced degradation by mt5 Drosha. HEK293T cells after transfection were exposed to heat (45°C, 45 min) or H_2O_2 (400 μM, 8 h) and blotted for Drosha. See also Figure S4.

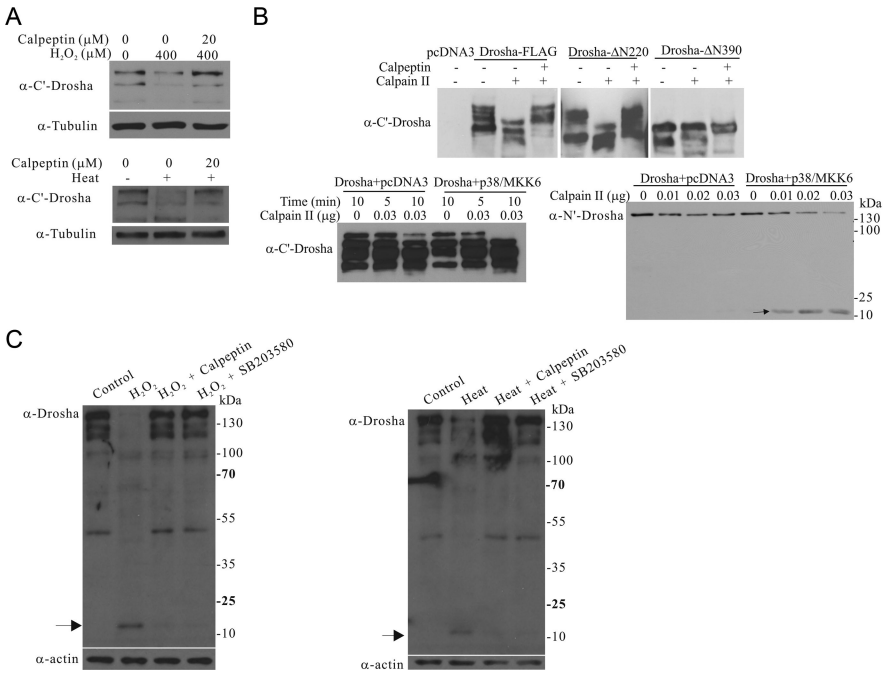

Figure 5.

Stress-induced cleavage of Drosha by calpain. **(A)** Effects of inhibition of calpain on stress-induced degradation of Drosha. HEK293T cells were pre-treated with calpain inhibitor calpeptin (20 μM) for 2 h and then exposed to H_2O_2 (400 μM, 6 h) or heat (45°C, 45 min). **(B)** Direct cleavage of Drosha by calpain. Drosha-FLAG wt, Δ N220, or ΔN390 immunoprecipitated from HEK293T cells was incubated with purified calpain II (0.05 μg) with or without calpeptin (20 μM) for 5 min at room temperature (top panel). Bottom panels show the levels of Drosha immunoprecipitated from transfected HEK293T cells after incubation with calpain II at 0°C. Arrow indicates the cleaved fragment. **(C)** The cleavage of Drosha after stress. HEK293T cells were pre-treated with the calpain inhibitor calpeptin (20 μM) or the p38 inhibitor SB203580 for 2 h and then exposed to H_2O_2 (400 μM, 6 h) or heat (45°C, 45 min). The lysates were blotted with anti-Drosha antibody. Arrow indicates the cleaved small fragment.

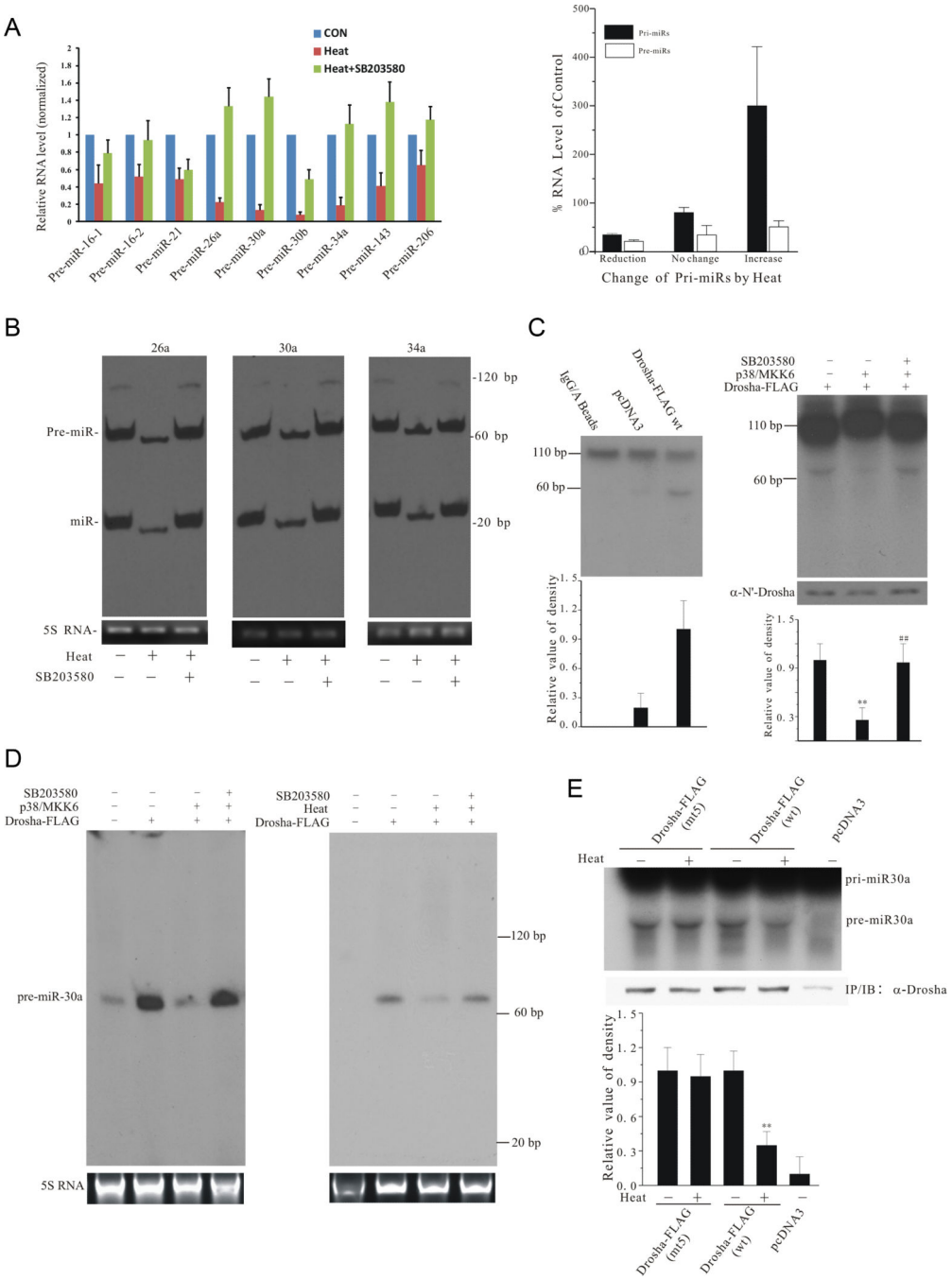

Figure 6.

Stress- and p38 MAPK-induced loss of Drosha function. **(A)** Heat-induced decrease in the levels of endogenous pre-miRNAs. HEK293T cells were treated with SB203580 or vehicle for 30 min, exposed to heat (45°C, 45 min), and re-cultured at 37°C for 3 h. Left panel shows the levels of endogenous pre-miRNAs determined by qRT-PCR in PureLink isolation kit prepared samples. Right panel shows the levels of the corresponding pri-miRNAs determined by qRT-PCR in TRIzol prepared samples (levels of pri- or pre-miRNAs without heat treatment were set as 100%. Reduction: pri-miRs 30b, 26a, and 34a; no change: pri-

miRs 16-1, 30a, and 21; increase: pri-miRs 16-2, 143, and 206). Primers used for qRT-PCR are listed in tables in supplementary experimental procedures. **(B)** Heat-induced loss of endogenous pre- and mature miRNAs. RNA (5 μg) purified by PureLink isolation kit from cells treated as in 6A was analyzed using Highly Sensitive MiRNA Northern Blot Kit (Signosis) and probes (sequences in supplementary experimental procedures). **(C)** p38 MAPK-induced loss of pri-miR-30a processing *in vitro*. Internally labeled pri-miR-30a probe was incubated with immunoprecipitated wt Drosha-FLAG (left) or with the total extracts prepared from HEK293T cells transfected as indicated (right). The bottom graphs show the quantification of pre-miR-30a levels (mean ± SEM, n = 3; **$p < 0.01$ vs Drosha alone group; $^{\#\#}p < 0.01$ vs Drosha/p38/MKK6 group). **(D)** p38 MAPK-dependent loss of pri-miR-30a processing in cells. Left panel: HEK293T cells transfected with pCMV-miR-30a and additional plasmids as indicated were treated with SB203580 for 12 h before the total RNA isolation. The levels of premiR-30a were analyzed by Northern blot with probe for pre-miR-30a (bottom panel shows 5S RNA as loading control). Right panel: Heat-induced loss of pri-miR-30a processing in cells. HEK293 cells transfected with pCMV-miR-30a were treated with SB203580 or vehicle for 30 min and exposed to heat (45°C, 45 min). The levels of pre-miR-30a were determined as in left panel. **(E)** Resistance to heat-induced inhibition of pri-miR-30a processing by mt5 Drosha. HEK293 cells transfected as indicated were exposed to heat as described in (D). Comparable amounts of Drosha-FLAG were immunoprecipitated and assessed for pri-miR-30a conversion as described in (C). The bottom panel is the quantification of pre-miR-30a levels (mean ± SEM, n = 3; **$p < 0.01$ vs Drosha alone group). See also Figure S5.

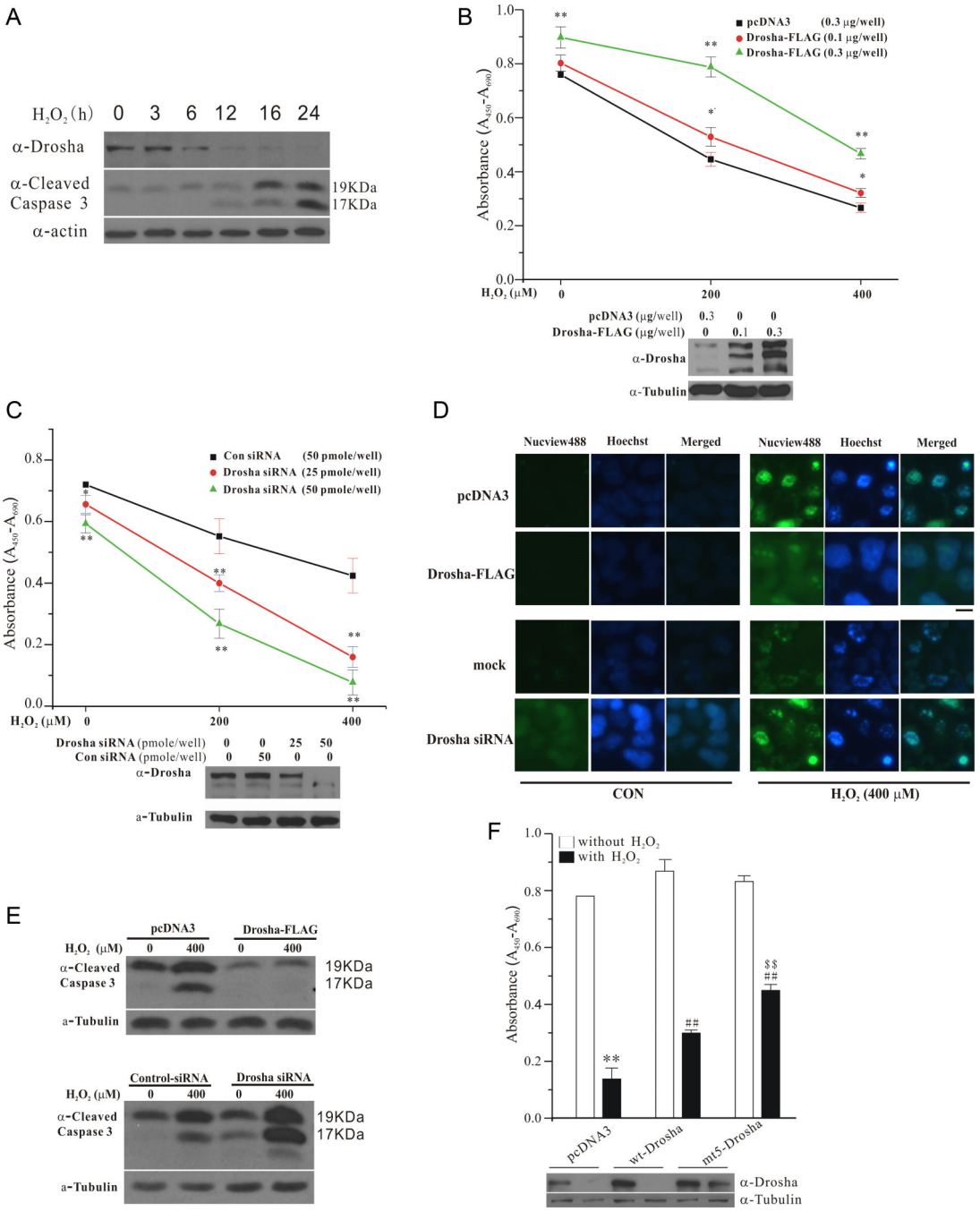

Figure 7.

Role of Drosha in cell survival. **(A)** Time-dependent change of Drosha and cleaved caspase 3 by H_2O_2. HEK293 cells treated with H_2O_2 (400 μM) were blotted with anti-Drosha and anti-cleaved caspase 3 anti-bodies. **(B)** Drosha-mediated protection against H_2O_2-induced death. HEK293T cells in 24-well plate were transfected with Drosha-FLAG (0.1 or 0.3 μg/well) for 24 h and treated with H_2O_2 (400 μM) for 24 h. Cell viability was measured by WST-1 assay (mean ± SEM, *p<0.05, **p<0.01 versus pcDNA3 in the same group, ANOVA and Tukey's test). Bottom panel shows the levels of over-expressed Drosha-FLAG.

(C) Increased sensitivity to H_2O_2-induced death by Drosha knockdown. HEK293T cells in 24-well plate transfected with control or Drosha siRNA (25 or 50 pmole/well) for 60 h were treated with H_2O_2 for 12 h. Cell viability was determined as described in (B) (mean ± SEM, *p<0.05, **p<0.01 versus Con siRNA in the same group, ANOVA and Tukey's test). Bottom panel is the levels of endogenous Drosha after knockdown. **(D)** Inhibition of stress-induced activation of caspase 3 by Drosha. HEK293T cells were transfected with control, Drosha-FLAG (0.3μg/well) or Drosha siRNA (50 pmole/well) as described in (C) for 24 h and treated with H_2O_2 (400 μM) (12 h for Drosha-FLAG and 8 h for Drosha siRNA). Activated caspase 3 in live cells was detected by a green fluorescent substrate probe (Biotium). The staining and imaging conditions were consistent throughout the experiment with a 200 ms and 10 ms exposure time for caspase and Hoechst (blue), respectively. The scale bar represents 10 μm. **(E)** Correlation of caspase 3 activity and Drosha by immunoblotting. HEK293T cells were treated as described in (D). The levels of active (cleaved) caspase 3 were determined by immunoblotting. (**F**) Effects of mt5 Drosha on cell survival. HEK293T cells after transfection were treated with H_2O_2 (400 μM) for 36 h. Cell viability was assessed by WST-1 (mean ± SEM; **p<0.01 vs pcDNA3 alone; $^{\#\#}$p<0.01 vs pcDNA3 treated with H_2O_2; $^{\$\$}$p<0.01 vs wt Drosha group treated with H_2O_2, ANOVA and Tukey's test). Western blot shows the level of expressed Drosha. See also Figure S6.